Proc. Natl. Acad. Sci. USA
Vol. 96, pp. 7029–7034, June 1999
Neurobiology

"Global" cell replacement is feasible via neural stem cell transplantation: Evidence from the dysmyelinated *shiverer* mouse brain

(myelination/mutants/oligodendroglia/regeneration)

BOOMA D. YANDAVA, LORI L. BILLINGHURST, AND EVAN Y. SNYDER*

Departments of Neurology, Pediatrics, and Neurosurgery, Harvard Medical School and Children's Hospital, Boston, MA 02115

Communicated by Richard L. Sidman, Harvard Medical School, Southborough, MA, April 6, 1999 (received for review February 23, 1999)

ABSTRACT **Many diseases of the central nervous system (CNS), particularly those of genetic, metabolic, or infectious/inflammatory etiology, are characterized by "global" neural degeneration or dysfunction. Therapy might require widespread neural cell replacement, a challenge not regarded conventionally as amenable to neural transplantation. Mouse mutants characterized by CNS-wide white matter disease provide ideal models for testing the hypothesis that neural stem cell transplantation might compensate for defective neural cell types in neuropathologies requiring cell replacement throughout the brain. The oligodendrocytes of the dysmyelinated *shiverer* (*shi*) mouse are "globally" dysfunctional because they lack myelin basic protein (MBP) essential for effective myelination. Therapy, therefore, requires widespread replacement with MBP-expressing oligodendrocytes. Clonal neural stem cells transplanted at birth—using a simple intracerebroventricular implantation technique—resulted in widespread engraftment throughout the *shi* brain with repletion of MBP. Accordingly, of the many donor cells that differentiated into oligodendroglia—there appeared to be a shift in the fate of these multipotent cells toward an oligodendroglial fate—a subgroup myelinated up to 52% (mean = ≈40%) of host neuronal processes with better compacted myelin of a thickness and periodicity more closely approximating normal. A number of recipient animals evinced decrement in their symptomatic tremor. Therefore, "global" neural cell replacement seems feasible for some CNS pathologies if cells with stem-like features are used.**

Many diseases of the central nervous system (CNS) are characterized not by discrete, focal neuropathology but, rather, by extensive, multifocal, or even "global" neural degeneration or dysfunction. Such conditions may require widespread replacement not only of therapeutic molecules, such as enzymes, but of neural cells, as well. "Global" cellular replacement has been regarded as beyond the capabilities of neural transplantation, which previously has been used in situations in which grafts are placed in single, relatively circumscribed, anatomic locations (e.g., the striatum in Parkinsonism). However, we previously demonstrated that neural stem cells (NSCs) can disseminate therapeutic gene products throughout the CNS (1, 2). We hypothesized that transplantation of NSCs also might work in situations requiring "global" replacement of degenerated or dysfunctional neural cells.

An NSC is an immature, uncommitted cell that exists in the developing and even adult nervous system and gives rise to the array of more specialized cells of the CNS (3–15). It is defined by its ability to self-renew, to differentiate into cells of most (if not all) neuronal and glial lineages, and to populate developing or degenerating CNS regions. The recognition that NSCs, propagated in culture, could be reimplanted into mammalian brain, where they could reintegrate appropriately and stably express foreign genes (1–9), provided hope that their use might make feasible a variety of novel therapeutic strategies. When exogenous NSCs are transplanted into germinal zones, they circumvent the blood–brain barrier, migrate to distant CNS regions, and participate in the normal development of multiple regions throughout the brain and at multiple stages (from fetus to adult), integrating seamlessly within the parenchyma, differentiating appropriately into diverse neuronal and glial cell types. Thus, their use as graft material can be considered almost analogous to hematopoietic stem cell-mediated reconstitution of bone marrow. In one of their earliest uses as a therapeutic tool, NSCs were implanted at birth, using a simple, rapid, intracerebroventricular injection technique. They delivered a missing gene product (β-glucuronidase) throughout the brain of a mouse in which the gene was mutated in all cells (the MPS VII mutant, a model of the neurodegenerative lysosomal storage disease mucopolysaccharidosis type VII), cross-correcting the widespread neuropathology of host neurons and glia by creating virtually chimeric brain regions (1). We hypothesized that a similar method might accomplish "global" replacement of degenerated or dysfunctional neural cells.

Mutant mice characterized by CNS-wide white matter disease because of oligodendrocyte dysfunction provide ideal models for testing this hypothesis. The *shiverer* (*shi*) mouse suffers from extensive dysmyelination because of an autosomal recessive defect that renders its oligodendrocytes dysfunctional in homozygous animals: a deletion of five of seven exons comprising the gene encoding myelin basic protein (MBP) makes the cells incapable of producing this oligodendroglial component that is essential for effective compact myelination (16–20). Severe tremors develop by 2–3 weeks of age. Therapy for this cell-autonomous defect would require extensive replacement with functional MBP-producing oligodendrocytes. (In a sense, replacement of both an abnormal neural cell type and a dysfunctional gene is entailed.) It is known that the *shi* cellular and behavioral phenotypes can be rescued by introducing the wild-type MBP gene into the germ line (17). However, this approach is not applicable to clinical therapies. The *shi* phenotype has been treated in discrete regions by injecting a fragment of primary CNS tissue containing normal, mature, MBP-expressing oligodendrocytes (19) in much the same way as other relatively focal, demyelinated lesions have been addressed by cells from various stages within the oligodendrocyte lineage (21, 22). However, this does not correct the global abnormality of *shi* CNS myelin. The most differentiated oligodendrocytes migrate minimally from the injection site, whereas cells that migrate more broadly are less

The publication costs of this article were defrayed in part by page charge payment. This article must therefore be hereby marked "*advertisement*" in accordance with 18 U.S.C. §1734 solely to indicate this fact.

PNAS is available online at www.pnas.org.

Abbreviations: CNS, central nervous system; NSC, neural stem cell; X-gal, 5-bromo-4-chloro-3-indolyl β-D-galactoside; β-gal, β-galactosidase; LM, light microscopy; EM, electron microscopy.

*To whom reprint requests should be addressed at: Harvard Medical School, Children's Hospital, 300 Longwood Avenue, 248 Enders Building, Boston, MA 02115. e-mail: Snyder@A1.TCH.Harvard.Edu.

likely to differentiate into mature myelinating cells (23). In contrast to resident oligodendrocytes and more differentiated precursors, multipotent, migratory NSCs tend not to differentiate until instructed by regional cues. This property might circumvent these problems. Therefore, NSCs were transplanted at birth into the brains of *shi* mutants, using the same intracerebroventricular implantation technique devised for diffuse engraftment of enzyme-expressing NSCs to treat global metabolic lesions (1, 2).

MATERIALS AND METHODS

Animals. *Shi* breeders were obtained initially from The Jackson Laboratory, and a colony was maintained thereafter in our facility. With careful husbandry, homozygous *shi* males and females (2–5 months of age) can mate with each other; a *shi*/*shi* genotype was ensured by using the progeny of such homozygous matings.

Transplantation. On the day of birth, *shi*/*shi* pups (and unaffected controls) received bilateral intracerebroventricular injections of a suspension of NSCs (clone C17.2) as described (1, 2). C17.2 is a stable, prototypical NSC clone originally derived from neonatal mouse cerebellum but capable of participating in the development of most other regions upon implantation into germinal zones throughout the brain (1, 2, 6, 24–26). The NSCs differentiate into neurons in regions undergoing neurogenesis or into glia, where gliogenesis is ongoing (6, 24, 25). Therefore, they emulate endogenous NSCs as well as NSC clones propagated by a variety of techniques from other structures (3–15). After 0–2 mitoses in the first 48 hr posttransplant, they become quiescent and intermingle nondisruptively with endogenous progenitors. The total cell number per region (host plus donor) is not increased. The clone constitutively and stably expresses *lacZ* [encoding β-galactosidase (β-gal), detectable by the 5-bromo-4-chloro-3-indolyl β-D-galactoside (X-gal) histochemical reaction]. Undifferentiated NSCs, maintained in culture and prepared for transplantation as detailed elsewhere (1, 2, 24–26), were resuspended in PBS at 4×10^4 cells/μl. The lateral ventricles of cryoanesthetized pups were visualized by transillumination of the head (1, 2); 2 μl of the cellular suspension was expelled gently via a glass micropipette inserted transcutaneously into each ventricle (gaining access to the subventricular zone). Pups were returned to maternal care until weaning. Six homozygous litters of eight offspring each were transplanted.

Analysis of Engrafted Brains. At various intervals between 2 and 8 weeks after transplantation, serial coronal sections of recipient brains were processed with X-gal histochemistry and/or an anti-β-gal antibody (Cappel, 1:1,000) to detect *lacZ*-expressing donor-derived cells as detailed previously (25, 27). The phenotypes of those cells were assessed by light microscopy (LM), immunocytochemistry, and electron microscopy (EM) by using predesignated, standard criteria detailed elsewhere (24–30). Although donor NSCs give rise to a range of neurons and glia *in vivo* [as in our previous reports (1, 2, 24–27)], this study was confined to an assessment of donor-derived oligodendroglia and their potential replacement; therefore, for the purposes of this study, all cells, both donor and host, were classified as either "oligodendrocytes" or "not oligodendrocytes." Because multiple modes of analysis could be performed on the same tissue, multiple parameters could be correlated in the same animal.

Morphologic analysis first was performed at the LM level by using bright-field, differential interference contrast (DIC) and/or immunofluorescence microscopy. Engrafted cells then were assessed by using ultrastructural criteria by EM for the direct visualization and quantitative morphometrics of cell type-specific components, including myelin (24–30). X-gal-processed tissue was prepared for EM as detailed previously (24–26). The X-gal reaction product forms a crystalline blue precipitate that is nondiffusible and electron dense, permitting donor-derived *lacZ*-expressing cells to be identified and distinguished unequivocally from unlabeled endogenous cells at both LM and EM levels (24–30) (see Figs. 4*D* and 5*A*). The precipitate typically is localized to the nuclear membrane, forming a nuclear ring within donor-derived cells (often overlying the nucleus), endoplasmic reticulum (ER), and other cytoplasmic organelles, and it frequently extends into cellular processes. Despite the presence of accepted LM features and immunocytochemistry markers, CNS cell types, and, particularly, functional oligodendrocytes, have been most extensively and reliably characterized ultrastructurally. Established criteria for cell-type assignment [detailed elsewhere (16–30)] were used. We also have validated independently these criteria by correlating ultrastructural, histologic, and antigenic profiles of individual donor-derived and host cells as detailed previously (24–30). Briefly, a cell was scored as an "oligodendrocyte" if it possessed the following ultrastructural criteria: was a small (5- to 8-μm diameter), round or oval cell with a smooth, regular perikaryon and a distinctively dark nucleus and cytoplasm (an appearance created by numerous fine granules); possessed a large, prominent nucleus (occupying more than one-half of the area of the cell) with dense heterochromatin marginated against the nuclear membrane and/or clumped centrally; possessed a thin rim of cytoplasm that, though not voluminous, could appear as a mass at the cellular poles when the nucleus lay eccentrically; and possessed a moderate number of short, round mitochondria and often long, meandering, distended ER (16–24, 28–30). Association with myelinated fibers, if visible in the same plane of section, helped confirm an oligodendroglial phenotype. Cells not meeting these criteria were scored as "nonoligodendrocytes."

Morphometric analysis of myelin on electron micrographs entailed assessment of the degree of compaction, including noting the presence of major dense lines (MDLs) (the oligodendroglial cytoplasmic membrane appositions that constitute the wraps of myelin) and quantifying both periodicity (a measure of interlamellar distance between myelin wraps as represented by the distance between intraperiod lines and/or MDLs) and width of the total myelin wrap. Measurements in engrafted regions of *shi* cerebrum were compared with those in unengrafted areas of the same mouse (internal control) and with those in analogous, homotopic regions of the cerebra of age-matched affected and unaffected, unengrafted control mice. Cell counts and morphometrics were performed under EM on randomly, systematically selected representative fields and EM grids from multiple noncontiguous sections spanning the cerebra of experimental and control mice. Cell-type assignments were confirmed independently by three observers blinded to the experiment.

The presence of MBP *in vivo* classically has been used in grafting studies into *shi* (31) to distinguish normal donor from mutant oligodendrocytes. For immunocytochemistry analysis of brain tissue, 20-μm-thick, 4% paraformaldehyde-fixed cryosections or 10-μm-thick, paraffin-embedded sections were reacted with a polyclonal antibody raised in rabbit against MBP (gift of D. Colman, Mt. Sinai; 1:200) by using standard immunoperoxidase (Vectastain, Vector Laboratories) or immunofluorescence procedures as detailed previously (2, 24, 25, 27). For analysis of cultured cells, a cellular monolayer was processed by using standard immunoperoxidase techniques. NSC-derived cells expressed MBP in culture after prolonged periods *in vitro* (>2 weeks) and/or after supplementation with conditioned medium from primary cultures of dissociated mouse cerebrum, a condition that appears to emulate the stably engrafted state.

Western Blot Analysis. Western blot analysis, using standard techniques and the above-referenced anti-MBP antibody, was performed on myelin-enriched membrane fractions (32) of whole-brain lysates prepared from semiserial coronal sections of transplanted *shi*/*shi* mice at 4–5 weeks of age, as well as age-matched, untransplanted *shi*/*shi* and unaffected controls.

Behavioral Assessment. Functional improvement in representative recipient animals was assayed by quantifying the amount of tremor by (*i*) scoring recorded cage behavior and (*ii*) measuring

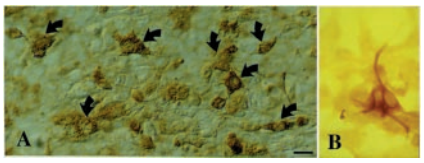

FIG. 1. NSCs can express MBP. Two engraftable NSC clones, known to give rise to oligodendrocytes *in vivo* after transplantation, are reacted with an antibody to MBP *in vitro* by using immunoperoxidase methodology. (*A*) A subpopulation of NSC clone C17.2 (arrows) differentiates into MBP-expressing cells after exposure to conditioned medium from a primary culture of newborn mouse forebrain. (*B*) Cells from clone C27.3 that spontaneously differentiated toward MBP expression. The present experiments were performed by using clone C17.2 because of prior experience with these cells in CNS-wide gene therapy engraftment paradigms.

the amplitude of tail tremor, a readily accessible, reliable, and reproducible measure of whole-body tremor.

Cage behavior of both transplanted ($n = 10$) and untransplanted ($n = 3$) affected mice as well as unaffected controls ($n = 3$) was videotaped and graded independently by three investigators blinded to the experiment. A four-point neurologic scoring scale was used, where a score of "1" corresponded to completely abnormal behavior and a score of "4" denoted a completely normal neurologic exam. Animals were rated according to their (*i*) exploring/grooming behavior, (*ii*) voluntary movement, (*iii*) tail movement and degree of tremor, and (*iv*) proprioception, coordination, and posture. Unaffected control mice, on this blinded assessment, achieved a mean score of 3.91 ± 0.14, which was significantly different from the mean score of 2.09 ± 0.08 received by untransplanted *shi* mutant controls ($P < 0.00001$), suggesting the sensitivity and validity of this assay with minimal interobserver variability. Each experimental animal similarly was graded blindly. At the completion of the study, upon breaking of the animals' identity codes, each score was calculated for a statistically significant difference from unaffected and affected/untreated animals. Mean scores of the groups also were compared.

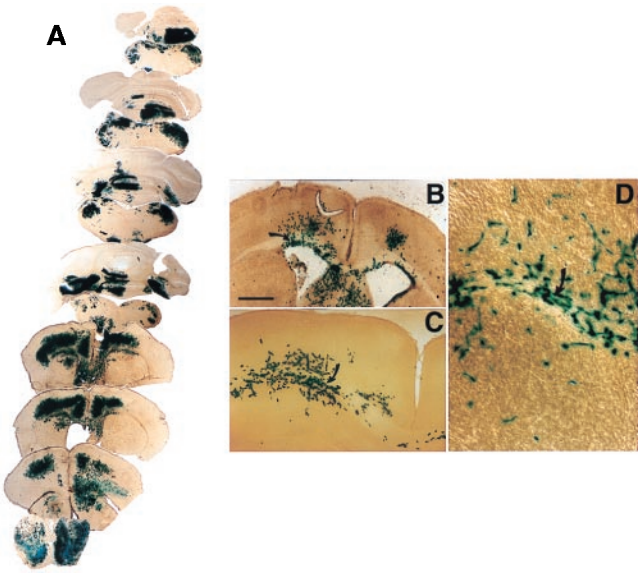

FIG. 2. NSCs engraft extensively throughout the *shi* dysmyelinated brain, including within white tracts. *LacZ*-expressing NSCs were transplanted into newborn *shi* mutants and analyzed systematically at intervals between 2 and 8 weeks after engraftment. (*A*) Semiserial coronal sections through the *shi* brain at adulthood demonstrate widely disseminated integration of blue X-gal$^+$ donor-derived cells throughout the neuraxis. (*B–D*) Progressively higher magnification of donor-derived cell integration in white tracts (arrows) at 2 weeks of age.

Because tremor is the most prominent feature of the *shi* behavioral phenotype, it was quantified directly by measuring the degree of tail displacement perpendicularly from a straight line drawn in the direction of the animal's forward movement (tail amplitude) (see Fig. 6 *C* and *D*). Measurements were made by coating an animal's tail in India ink and then permitting the mouse to move freely in one direction on a sheet of graph paper. The tail of an unaffected nontremulous animal draws a line with virtually no perpendicular displacement from the direction of movement (i.e., the long axis of the body); e.g., amplitude = 0 cm. The tail of a "shivering" animal demarcates a broad region of movement (tremor) about the line (i.e., displacement perpendicular to that axis; e.g., amplitude = 4 cm).

RESULTS AND DISCUSSION

The use of NSCs to address the widespread oligodendroglial pathology of the *shi* CNS was predicated on three observations: (*i*) our previous determination that NSC clones are capable of differentiating into morphologically, immunocytochemically, and ultrastructurally proven oligodendrocytes *in vitro* and *in vivo* after transplantation into wild-type mouse brain (2, 6, 24, 25, 27); (*ii*) our confirmation at the outset of these experiments that they are capable of producing MBP (Fig. 1); and (*iii*) our prior experience that the implantation and integration of exogenous NSC clones into germinal zones of fetuses and newborns (1, 2, 26, 27) could ensure their dissemination throughout a recipient's brain, with normal development of the virtually chimeric regions to which they contribute.

Therefore, clonal NSCs were transplanted at birth into the brains of *shi* mice (as well as unaffected controls), using the same intracerebroventricular implantation technique devised previously for the widespread engraftment of enzyme-expressing NSCs to treat global metabolic lesions (1, 2). Within 24 hr after implantation, consistent with our prior observations (1, 2, 27),

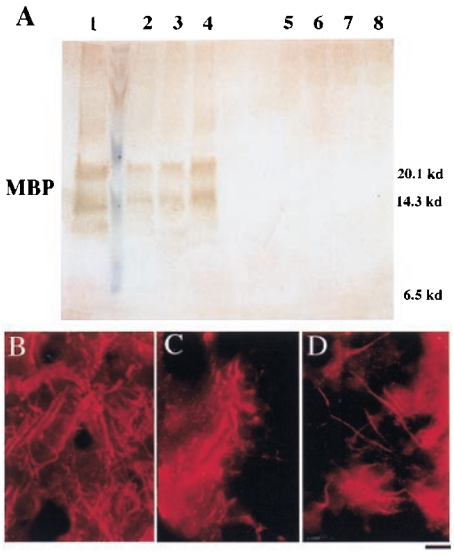

FIG. 3. MBP expression in mature transplanted and control brains. (*A*) Western analysis for MBP in whole-brain lysates. The brains of three representative transplanted *shi* mutants (lanes 2–4) express MBP at levels close to that of an age-matched, unaffected mouse (lane 1, positive control) and significantly greater than the amounts seen in untransplanted (lanes 7 and 8, negative control) or unengrafted (lanes 5 and 6, negative control), age-matched *shi* mutants. (Identical total protein amounts were loaded in each lane.) (*B–D*) Immunocytochemical analysis for MBP. (*B*) The brain of a mature unaffected mouse is immunoreactive to an antibody to MBP (revealed with a Texas Red-conjugated secondary antibody). (*C* and *D*) Age-matched engrafted brains from *shi* mice similarly show immunoreactivity. Untransplanted *shi* brains lack MBP. Therefore, MBP immunoreactivity also classically has been a marker for normal, donor-derived oligodendrocytes (*C* and *D*) in transplant paradigms (31).

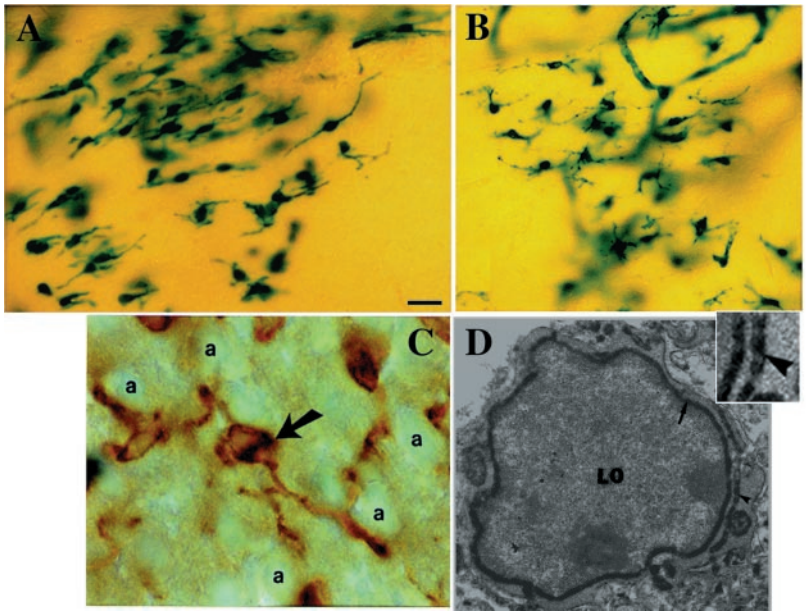

FIG. 4. Engrafted NSCs in recipient *shi* mutants differentiate into oligodendrocytes. (*A* and *B*) Donor-derived X-gal$^+$ cells in representative sections through the corpus callosum possess characteristic oligodendroglial features (small, round or polygonal cell bodies with multiple fine processes oriented in the direction of the neural fiber tracts). (*C*) Close-up of a representative donor-derived anti-β-gal immunoreactive oligodendrocyte (arrow) extending multiple processes toward and beginning to enwrap large, adjacent axonal bundles ("a") viewed on end in a section through the corpus callosum. That cells such as those in *A–C* (and in Fig. 3 *C* and *D*) are oligodendroglia is confirmed by the representative electron micrograph in *D* (and in Fig. 5*A*), demonstrating the defining ultrastructural features detailed in *Materials and Methods*. A donor-derived X-gal-labeled oligodendrocyte ("LO") can be distinguished by the electron-dense X-gal precipitate that typically is localized to the nuclear membrane (arrow), endoplasmic reticulum (arrowhead), and other cytoplasmic organelles. The area indicated by the arrowhead is magnified in the *Inset* to demonstrate the unique crystalline nature of individual precipitate particles.

NSCs integrated within the subventricular zone throughout the length of the ventricular system and, by 1–2 weeks posttransplant, had migrated into and engrafted extensively within the *shi* brain parenchyma (Fig. 2). At maturity, *lacZ*$^+$ donor-derived cells were integrated seamlessly throughout the *shi* neuraxis (Fig. 2*A*), including within white tracts (Fig. 2 *B–D*). The brains of transplanted *shi* mutants, as assessed by Western analysis of whole-brain lysates (Fig. 3*A*), now expressed readily detectable levels of MBP (lanes 2–4) that contrasted markedly with the absence of MBP in unengrafted, age-matched *shi* brains (lanes 5–8) and compared favorably with that present in unaffected brains (lane 1). Immunocytochemistry analysis using an antibody to MBP (Fig. 3 *B–D*) (31) confirmed expression of MBP at the cellular level in engrafted *shi* brains (Fig. 3 *C* and *D*) with an immunoreactivity comparable to that in nonmutant brains (Fig. 3*B*). Therefore, transplantation of NSCs into the MBP-deficient *shi* brain resulted in widespread engraftment with repletion of significant amounts of whole-brain MBP.

This observation lent support to the expectation that, had donor NSCs indeed differentiated into mature, normal oligodendrocytes, then they would effectively enwrap host axons and dendrites with better-compacted myelin. The phenotype of transplanted NSCs, therefore, was confirmed by LM and EM.

Under bright field, such donor-derived, *lacZ*$^+$ cells, particularly within white tracts, indeed possessed a morphology classic for

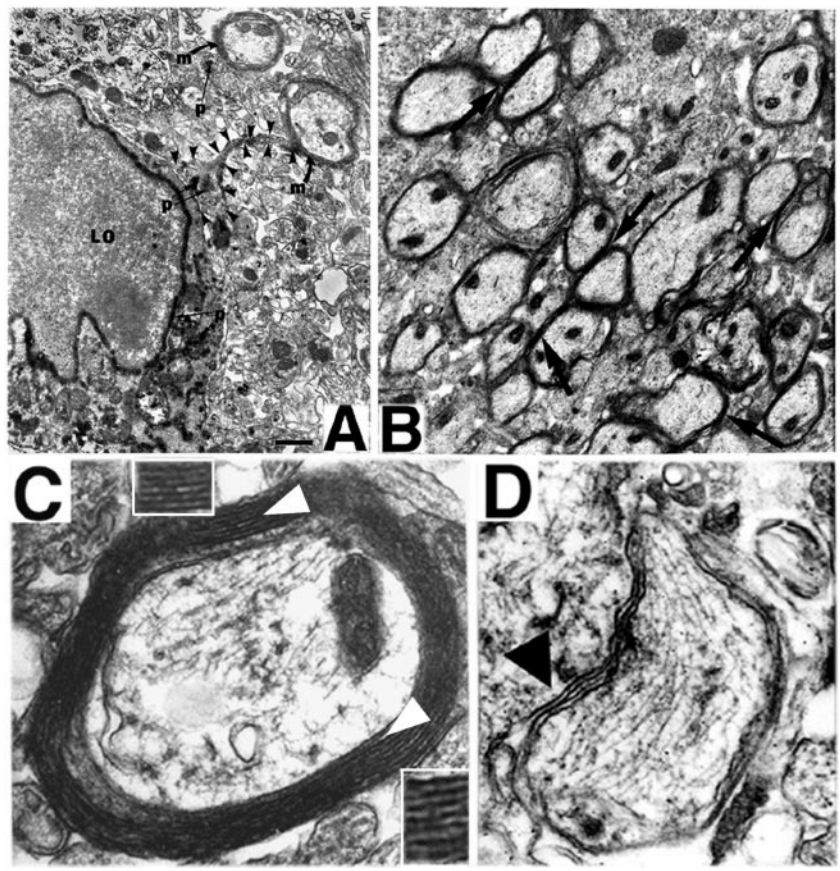

FIG. 5. NSC-derived "replacement" oligodendrocytes appear functional as demonstrated by ultrastructural evidence of myelination of *shi* axons. In regions of MBP-expressing NSC engraftment, *shi* neuronal processes become enwrapped by thick, better-compacted myelin. (*A*) At 2 weeks posttransplant, a representative donor-derived, labeled oligodendrocyte ("LO") [recognized by extensive X-gal precipitate ("p") in the nuclear membrane, cytoplasmic organelles, and processes] is extending processes (a representative one is delineated by arrowheads) to host neurites and is beginning to ensheathe them with myelin ("m"). (*B*) If engrafted *shi* regions, such as that in *A*, are followed over time (e.g., to 4 weeks of age as pictured here), the myelin begins to appear healthier, thicker, and better compacted (examples indicated by arrows) than that in age-matched, untransplanted control mutants. (*C*) By 6 weeks posttransplant, these mature into even thicker wraps; ≈40% of host axons are ensheathed by myelin (a higher-power view of a representative axon is illustrated in *C*) that is dramatically thicker and better compacted than that of *shi* myelin [an example of which is shown in *D* (black arrowhead) from an unengrafted region of an otherwise successfully engrafted *shi* brain]. In *C*, open arrowheads indicate representative regions of myelin that are magnified in the adjacent respective *Insets*; major dense lines are evident.

Table 1. Morphometric and behavioral analysis

Parameter	Normal	Shiverer	
		Unengrafted	Engrafted
Neuronal processes with myelin and MDLs,* %	96.7	0	37.8
Periodicity of myelin,† nm	4.5 ± 0.2	24.4 ± 5.8	10.5 ± 0.7
Width of myelin wrap, nm	138 ± 5	59.5 ± 1.5	135 ± 20
Degree of tremor (as tail displacement,‡ cm	0	4	1.2 ± 1.6
Behavioral score§ (scale = 1–4)	3.91 ± 0.14	2.09 ± 0.08	3.72 ± 0.20

*MDLs, major dense lines, an indication of compacted myelin; the data represent the mean percentage of axons and dendrites with MDLs in representative specimens examined.

†See *Materials and Methods* for definition. The shorter the distance, the better compacted and, hence, more normal the myelin.

‡See "Behavioral Assessment" in *Materials and Methods* as well as Fig. 6 *C* and *D* for a description. Zero centimeter of tail displacement suggests minimal to no tremor; 4 cm of displacement reflects extensive tremor. Of the 10 transplanted *shi* mice examined, 6 actually showed zero displacement.

§See "Behavioral Assessment" in *Materials and Methods* as well as Fig. 6 *A* and *B* for a description of the scoring system. Unengrafted *shi* mutants scored significantly worse than normal mice ($P < 0.0001$); the scores for successfully engrafted *shi* mice examined in this fashion, however, ($n = 6$) were statistically indistinguishable from those of normal mice ($P = 0.20$) and significantly better than unengrafted *shi* mice ($P < 0.0001$). Unsuccessfully transplanted *shi* mice ($n = 4$; mean score = 1.97 ± 0.29) were indistinguishable from untransplanted *shi* [i.e., significantly different from scores in the "normal" column ($P < 0.0003$), not statistically different from scores in the "unengrafted *shi*" column].

oligodendrocytes (Fig. 4 *A–C*), typically extending processes toward large axonal bundles (Fig. 4*C*). The crystalline X-gal precipitate is electron-dense, ensuring unambiguous designation and characterization of donor-derived cells even at the EM level (8, 24–30). EM analysis of x-gal+ donor-derived cells confirmed that they met the defining ultrastructural criteria of oligodendrocytes (e.g., Figs. 4*D* and 5*A*) (detailed in *Materials and Methods*).

Therefore, donor NSCs could differentiate into ultrastructurally confirmed oligodendrocytes in the engrafted *shi* brain. Of interest was the additional observation that, although these multipotent donor cells were able to differentiate into multiple neural cell types in the engrafted *shi* brains, a significantly greater percentage of engrafted NSCs differentiated toward an oligodendroglial phenotype in the *shi* brain (28%) than in normal controls (16%; $\chi^2 = 0.015$), suggesting that NSCs actually may be compensating somewhat specifically for oligodendrocyte dysfunction in *shi*. Of note, a similar shift in the fate of this same clone of multipotent NSCs toward a neuronal phenotype was detected in developing (26) and adult (25) mouse brain when that neural cell type was deficient or defective and required compensation. Taken together these observations suggest that NSCs might possess a mechanism whereby their differentiation is directed to replenish deficient or inadequate cell types. Such behavior may reflect a fundamental developmental strategy with therapeutic utility.

The successful repletion of MBP in the *shi* brain suggested that donor-derived oligodendrocytes should be functional and, hence, form healthier myelin throughout the brain. Indeed, as early as 2 weeks posttransplant, a subpopulation of donor-derived oligodendrocytes extended processes that enwrapped host axons and dendrites and began laying down myelin around neuronal processes (Fig. 5*A*). Over a period of 3–4 weeks, the myelin produced by these oligodendrocytes appeared healthier, thicker, and better compacted (Fig. 5*B*). By 6 weeks posttransplant, a mean of ≈40% of host neuronal processes (Table 1) (up to 52% in some representative specimens examined) were ensheathed by donor-derived myelin (Fig. 5*C*) that contrasted dramatically with that observed in untransplanted control mutants or even with that in unengrafted areas of successfully transplanted *shi* animals (Fig. 5*D*) (an internal control for the efficacy of engraftment) and that compared quite favorably with wild-type myelin. Morphometric analysis of myelinated neuronal processes in engrafted mutants confirmed that the periodicity of myelin was significantly closer to and the mean thickness of myelin virtually equaled ($P > 0.1$) that of normal controls (Table 1).

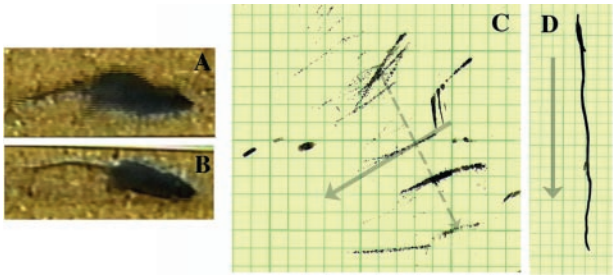

FIG. 6. Functional and behavioral assessment of transplanted *shi* mutants and controls. The *shi* mutation is characterized by the onset of tremor and a "shivering gait" by the second to third postnatal week. The degree of motor dysfunction in animals was gauged in two ways: (*i*) by blindly scoring periods of standardized videotaped cage behavior of experimental and control animals and (*ii*) by measuring the amplitude of tail displacement from the body's rostral–caudal axis (an objective, quantifiable index of tremor) (see *Materials and Methods*). Video freeze-frames of representative unengrafted and successfully engrafted *shi* mice are seen in *A* and *B*, respectively. The whole-body tremor and ataxic movement observed in the unengrafted symptomatic animal (*A*) causes the frame to blur, a contrast to the well focused frame of the asymptomatic transplanted *shi* mouse (*B*). The neurologic scoring of such mice is detailed in *Materials and Methods* and Table 1; 60% of transplanted mutants evinced nearly normal-appearing behavior as in *B* and attained scores that were not significantly different from normal controls. *C* and *D* depict the manner in which whole-body tremor was mirrored by the amplitude of tail displacement (hatched, gray arrow in *C*), measured perpendicularly from a line drawn in the direction of the animal's movement (solid, gray arrow, which represents the body's long axis) (see *Materials and Methods*). Measurements were made by permitting a mouse, whose tail had been dipped in India ink, to move freely in a straight line on a sheet of graph paper as shown. Large degrees of tremor cause the tail to make widely divergent ink marks away from the midline, representing the body's axis (*C*). Absence of tremor allows the tail to make long, straight, uninterrupted ink lines on the paper congruent with the body's axis (*D*). The distance between points of maximal tail displacement from the axis was measured and averaged for transplanted and untransplanted *shi* mutants and for unaffected controls (hatched, gray arrow). *C* shows data from a poorly engrafted mutant that did not improve with respect to tremor whereas *D* reveals lack of tail displacement in a successfully engrafted, now asymptomatic *shi* mutant. Overall, 64% of transplanted *shi* mice examined displayed at least a 50% decrement in the degree of tremor or "shiver." Several showed zero displacement (see Table 1).

The success of NSC transplantation in *shi* ultimately is determined by its ability to achieve functional improvement. To this end, transplanted mutants as well as unaffected (positive control) and untransplanted *shi* (negative control) mice were analyzed (as detailed in *Materials and Methods*) for functional improvement by (*i*) scored neurologic assessment during free-cage behavior and (*ii*) quantifying the degree of "shiver" as reflected in the amplitude of tail tremor. Behaviorally relevant tremors were decreased significantly in a significant number of representative recipient mutants (Fig. 6 and Table 1): 60% of tested transplanted mutants evinced behavior that approximated normal (Fig. 6*B*), i.e., attained neurologic scores that both individually and as a group mean were statistically indistinguishable from normal controls ($P > 0.1$) on the behavioral scale detailed in *Materials and Methods* (Table 1); 64% of transplanted animals showed at least a 50% decrement in measured tremor, and some engrafted animals evinced virtually no "shiver" (and, hence, essentially no

tail displacement) (Fig. 6*D*). This suggests that the "replacement cells" (in this case, oligodendrocytes) were integrated into host CNS in a functionally relevant manner.

The variability in behavioral improvement after engraftment does not have a simple explanation: there did not appear to be a simple correlation between functional improvement and the degree of NSC engraftment or MBP expression. Etiology of the "shivering" phenotype, however, is complex and not well understood. Symptomatic improvement may not be simply a measure of the overall amount of successful myelination. Instead, it may be more reflective of successful remyelination in specific CNS regions. Indeed, one hypothesis holds that there is a shivering "center" affected in *shi* mice. If this hypothesis holds, variations in experimental animals may represent the degree to which such a center was myelinated successfully. It is also important to note that we did not focus on addressing spinal cord defects in *shi*; these lesions likely mediate expression of symptoms as well. Despite the fact that we obtained significant NSC engraftment, MBP expression, oligodendrocyte differentiation, and myelination, it is likely that these could be optimized further: given that NSCs are so readily manipulated (5–8), future studies could use NSCs genetically engineered or pretreated (3, 6) *ex vivo* to enhance these capacities. It is also unclear which role donor-derived nonoligodendroglial cells might have played in effecting repair of the dysmyelinated *shi* brain. Neurons and astrocytes have been implicated in oligodendrocyte migration and differentiation and may influence myelination. The extent to which such other neural cell types, derived from the same clone of NSCs, may have had "helper" roles in improvement might constitute an additional argument for the use of multipotent cells rather than those with a more restricted fate. Indeed, many diseases—even those classically characterized as purely disorders of white or gray matter—actually affect a mixed population of cell types and would benefit from the concurrent replacement of both neuronal and glial elements.

Conclusions

Transplanted NSCs can differentiate into MBP-expressing oligodendrocytes throughout the *shi* brain, in turn promoting improved widespread remyelination with extensive amelioration of neuropathology and symptoms. These results suggest that NSCs may be useful for a variety of diseases characterized by profuse white matter degeneration that might benefit from the replacement of oligodendroglia. Disordered myelination plays an important role in many other genetic and acquired neurodegenerative processes. In a broader sense, with oligodendroglia serving as a model for neural cells in general and *shi* serving as a prototype for a broad range of maladies characterized by extensive neural cell dysfunction, these results suggest that therapeutic cell replacement in a widely disseminated, even "global," manner is feasible when cells with stem-like qualities are used as graft material, a recognition that broadens the paradigmatic scope of neural transplantation. Furthermore, an NSC-based approach, whether with exogenous NSCs or with appropriately mobilized endogenous NSCs, may address therapeutic challenges that previously have been inaccessible. Many promising gene therapy vehicles and biochemical treatment modalities depend on relaying "new" genetic information through "old" neural substrates that may, in fact, have been lost, become dysfunctional, or failed to develop. Reconstitution of aspects of this anatomy may enable more significant recovery. Furthermore, although the ability of NSCs to engraft diffusely has been exploited for widespread distribution of enzymes (1, 2) and, now, cells, it seems apparent that a similar strategy can be used for dissemination of a variety of diffusible (e.g., neurotrophins, viral vectors) (33) and nondiffusible (e.g., extracellular matrix) factors for a wide range of therapeutic and research demands. Combined therapies may forestall damage while restoring lost neural elements. NSCs with similar properties recently have been generated from human tissue, laying the groundwork for potential treatments of heretofore refractory human diseases (27, 34). The persistence of a periventricular zone in the human for prolonged periods postnatally suggests that implantation strategies similar to those described may be feasible.

We thank D. Kirschner, J. Karthegasen, R. Mozell, and R. M. Taylor for advice and D. Colman for his generous gift of MBP antibody. This work was supported in part by grants from the National Institute of Neurological Disorders and Stroke, the Hood Foundation, the American Paralysis Association, the Paralyzed Veterans of America, the Canavan's Research Fund, and a Mental Retardation Research Center grant to Children's Hospital. L.L.B. was funded in part by the Society for Pediatric Research.

1. Snyder, E. Y., Taylor, R. M. & Wolfe, J. H. (1995) *Nature (London)* **374,** 367–370.
2. Lacorazza, H. D., Flax, J. D., Snyder, E. Y. & Jendoubi, M. (1996) *Nat. Med.* **4,** 424–429.
3. McKay, R. (1997) *Science* **276,** 66–71.
4. Gage, F. H., Ray, J. & Fisher, L. J. (1995) *Annu. Rev. Neurosci.* **18,** 159–192.
5. Gage, F. H. & Christen, Y., eds. (1997) *Isolation, Characterization, and Utilization of CNS Stem Cells—Research and Perspectives in Neuroscience* (Springer, Berlin).
6. Snyder, E. Y. (1998) *Neuroscientist* **4,** 408–425.
7. Martinez-Serrano, A. & Bjorklund, A. (1997) *Trends Neurosci.* **20,** 530–538.
8. Whittemore, S. R. & Snyder, E. Y. (1996) *Mol. Neurobiol.* **12,** 13–38.
9. Pincus, D. W., Goodman, R. R., Fraser, R. A. R., Nedergaard, M. & Goldman, S. A. (1998) *Neurosurgery* **42,** 858–868.
10. Morrison, S. J., Shah, N. M. & Anderson, D. J. (1997) *Cell* **88,** 287–298.
11. Weiss, S., Reynolds, B. A., Vescovi, A. L., Morshead, C., Craig, C. & van der Kooy, D. (1996) *Trends Neurosci.* **19,** 387–393.
12. Alvarez-Buylla, A. & Lois, C. (1995) *Stem Cells* **13,** 263–272.
13. Qian, X., Davis, A. A., Goderie, S. K. & Temple, S. (1997) *Neuron* **18,** 81–93.
14. Kilpatrick, T. & Bartlett, P. F. (1993) *Neuron* **10,** 255–265.
15. Gritti, A., Parati, E. A., Cova, L., Frolichsthal, P., Galli, R., Wanke, E., Faravelli, L., Morassutti, D. J., Roisen, F., Nickel, D. D., *et al.* (1996) *J. Neurosci.* **16,** 1091–1100.
16. Molineaux, S. M., Engh, H., de Ferra, F., Hudson, L. & Lazzarini, R. A. (1986) *Proc. Natl. Acad. Sci. USA* **83,** 7542–7546.
17. Readhead, C., Popko, B., Takahashi, N., Shine, H. D., Saavedra, R. A., Sidman, R. L. & Hood, L. (1987) *Cell* **48,** 703–712.
18. Popko, B., Puckett, C., Lai, E., Shine, H. D., Readhead, C., Takahashi, N., Hunt, S. W., Sidman, R. L. & Hood, L. (1987) *Cell* **48,** 713–721.
19. Gout, O., Gansmuller, A., Baumann, N. & Gumpel, M. (1988) *Neurosci. Lett.* **87,** 195–199.
20. Katsuki, M., Sato, M., Kimura, M., Yokoyama, M., Kobayashi, K. & Nomura, T. (1988) *Science* **241,** 593–595.
21. Duncan, I. D., Grever, W. E. & Zhang, S.-C. (1997) *Mol. Med. Today* **3,** 554–561.
22. Franklin, R. J. M. & Blakemore, W. F. (1995) *Trends Neurosci.* **18,** 151–156.
23. Foster, L. M., Landry, C., Phan, T. & Campagnoni, A. T. (1995) *Dev. Neurosci.* **17,** 160–170.
24. Snyder, E. Y., Deitcher, D. L., Walsh, C., Arnold-Aldea, S., Hartwieg, E. A. & Cepko, C. L. (1992) *Cell* **68,** 33–51.
25. Snyder, E. Y., Yoon, C., Flax, J. D. & Macklis, J. D. (1997) *Proc. Natl. Acad. Sci. USA* **94,** 11663–11668.
26. Rosario, C. M., Yandava, B. D., Kosaros, B., Zurakowski, D., Sidman, R. L. & Snyder E. Y. (1997) *Development* **124,** 4213–4224.
27. Flax, J. D., Aurora S., Yang, C., Simonin, C., Wills, A. M., Billinghurst, L., Jendoubi, M., Sidman, R. L., Wolfe, J. H., Kim, S. U. & Snyder, E. Y. (1998) *Nat. Biotech.* **16,** 1033–1039.
28. Peters, A., Palay, S. L. & Webster, H. D. (1991) *The Fine Structure of the Nervous System, Neurons, and Their Supporting Cells* (Oxford Univ. Press, Oxford).
29. Jones, E. G. (1981) *The Structural Basis of Neurobiology* (Elsevier, New York).
30. Palay, S. L. & Chan-Palay, V. (1973) *J. Microsc. (Oxford)* **97,** 41–47.
31. Gumpel, M., Bauman, N., Raoul, M. & Jacque, C. (1983) *Neurosci. Lett.* **37,** 307–311.
32. Knapp, P. E., Bartlett, W. P. & Skoff, R. P. (1987) *Dev. Biol.* **120,** 356–365.
33. Lynch, W. P., Sharpe, A. H. & Snyder, E. Y. (1999) *J. Virol.,* in press.
34. Vescovi, A. L., Parati, E. A., Gritti, A., Poulin, P., Ferrario, M., Wante, E., Frolichsthal-Schoeller, P., Cova, L., Arcellana-Panlilio, M., Colombo, A. & Galli, R. (1999) *Exp. Neurol.* **156,** 71–83.